



CHORUS

This is the accepted manuscript made available via CHORUS. The article has been published as:

Antiferromagnetic coupling in EuO_{1-x}

Pan Liu and Jinke Tang

Phys. Rev. B **85**, 224417 — Published 15 June 2012

DOI: [10.1103/PhysRevB.85.224417](https://doi.org/10.1103/PhysRevB.85.224417)

Antiferromagnetic Couplings in EuO_{1-x}

Pan Liu and Jinke Tang*

Department of Physics and Astronomy, University of Wyoming, Laramie, WY 82071

ABSTRACT

The mechanism for the ferromagnetic order in oxygen-deficient europium monoxide EuO_{1-x} at temperatures higher than 69 K (the Curie temperature T_c of stoichiometric EuO) remains controversial. We have investigated the magnetization of EuO_{1-x} thin films prepared via pulsed laser deposition as a function of temperature and applied field. The ferromagnetic ordering above 69 K originates from the exchange coupling between the doped electrons and Eu 4f moments and is described using a magnetic polaron model. Our data show that the magnetic polarons are coupled antiferromagnetically to the Eu 4f local moments that dominate the magnetization below 69 K. The magnetic polaron state is stable below 69 K and seems to persist down to a relatively low temperature. An explanation is given to account for the antiferromagnetic coupling. We also describe the evolution of the phases of the magnetic orders as the temperature is varied in EuO_{1-x} .

I. INTRODUCTION

Europium chalcogenides EuX ($X = \text{O}, \text{S}, \text{Se}, \text{and Te}$) have been studied extensively since 1961¹ as the only clear realization of the Heisenberg ferromagnets.^{2,3} In particular, being a valuable ferromagnetic semiconductor with a band gap of about 1.12 eV,^{4,5} EuO receives a lot of attention due to its higher Curie temperature (T_c) of 69 K. It has a rock salt structure, with a lattice constant of 5.144 Å at room temperature.⁶ There are also some spectacular phenomena for this material with electron doping, such as a metal-to-insulator transition and colossal magnetoresistance, where the resistivity change can exceed 8-10 orders of magnitude,^{7,8} much stronger than the famous manganites. The Faraday rotation ($\sim 5 \times 10^5$ °/cm at 632.8 nm) of EuO is one of the highest of any known materials.⁹ Recent studies of spin-resolved x-ray absorption spectroscopy have shown a spin-split conduction band of about 0.6 eV in its ferromagnetic state, creating a nearly 100% spin polarized electrons close to the conduction band edge.¹⁰ Although the stoichiometric EuO has a Curie temperature (T_c) of 69 K, T_c can be enhanced significantly by pressure,¹¹⁻¹³ interfacial strain¹⁴ or electron doping via rare-earth atoms¹⁵⁻²⁴ or oxygen vacancies.^{15,16, 23-25} The integrations of EuO with Si ,^{18, 23-27} GaAs ,²⁸ and GaN ¹⁸ have been successfully demonstrated. These properties make EuO a very good candidate for device applications in the field of spintronics.

Although much effort has been devoted to this material, there are still several controversies with regard to its magnetic properties. Charge carrier doping by either oxygen vacancies^{15, 23-25} or substituting Eu^{2+} with trivalent rare earth elements such as Gd^{3+} ,^{15-17, 19, 21-23} Ce^{3+} ,²⁴ and La^{3+} ^{18,20} has been used to increase the T_c of EuO , often resulting in a unique double-dome feature in the $M(T)$ curves. Upon electron doping, the extra electrons are bound in defect levels situated in the semiconductor band gap, and the transition to a ferromagnetic metal occurs when the majority states of the spin-split conduction band shift downward to overlap with the defect levels.^{4,29} This view is widely accepted, but different models/theories have been proposed. Mauger suggested long ago the increased T_c is due to the enhancement of the magnetic

coupling between the 4f Eu^{2+} local moments mediated by the 5d conduction electrons that are excited from the defect states (a kind of RKKY interaction).³⁰ Oliver *et al.* presented a model (He-like model) to account for some of the properties in oxygen-deficient EuO ,⁷ in which a temperature-independent impurity level for the oxygen vacancies was proposed. It is below the conduction band at high temperatures but crossed by the spin-up conduction band as the temperature is decreased. Another model based on bound magnetic polaron (BMP) was used to explain the mechanism of oxygen-deficient EuO .³¹ An exchange interaction between the doped electrons due to oxygen vacancies and the localized Eu spins was assumed. Whether this exchange coupling is ferromagnetic or antiferromagnetic is still subject to debate.³²⁻³⁴ A Kondo-lattice model containing the impurity orbitals and their hybridization with the conduction band was also formulated for this topic.³⁵ According to Arnold and Kroha,²⁹ the existence of preformed local moments at the impurity levels inside the semiconducting gap is essential to explain the distinct double-dome shape of the magnetization $M(T)$, although it has become apparent from numerous experiments that oxygen deficiency alone, without doping localized moments, can be responsible for the unique double-dome feature.^{15,16,23-25} It should be pointed out that the double-dome feature is observed in single-phase clean samples and is an intrinsic property of electron doped EuO . A recent report found that the “dome” above 69 K is only observed for measurements performed at high magnetic fields and attributed it to the presence of paramagnetic Eu metal clusters.³⁶ This situation seems to be limited to the samples of that particular study as ferromagnetic ordering above 69 K is well established in electron doped samples although it is possible that their data signal the presence of isolated magnetic polarons to be discussed in this paper. Questions remain: what is the exact mechanism through which the T_c is enhanced by electron doping via rare-earth substitution or oxygen vacancies; and what is the difference in the nature of the ferromagnetically ordered states above 69 K and below it?

In this study, we have investigated the magnetic properties of oxygen-deficient

EuO thin films. Magnetization as a function of temperature and applied field shows clear indication for antiferromagnetic coupling between the magnetic moments dominant at temperatures $T > 69$ K and the Eu 4f local moments of the Heisenberg ferromagnet below 69 K. The coupling results in unique behaviors in the coercivity and inverted hysteresis loops in the vicinity of 69 K. We propose a model to account for the observed properties and suggest evolution of the phases of the magnetic orders as the temperature is varied in EuO_{1-x} .

This paper is organized as follows. In Sec. II, sample preparation and experimental details of the measurements are described. In Sec. III, we discuss the experimental results of the magnetic properties of oxygen-deficient EuO, in particular, the magnetization, hysteresis and coercivity as a function of temperature and applied field. Sec. IV gives the conclusions.

II. EXPERIMENTS

For samples grown on Si substrates, the Si wafers were cleaned with dilute HF acid and rinsed with acetone, and then immediately placed in the vacuum chamber. Before the deposition, the silicon wafers were annealed at a temperature of 750°C in a chamber of pure H_2 gas of pressure 10^{-5} Torr to remove the native SiO_2 surface layer from the wafers. The substrate temperature for growing oxygen deficient EuO is 300°C . Pulsed laser deposition was the method used to prepare the films. The targets were Eu (99.9%) metal from Alfa Aesar. And the purity of H_2 gas used during the deposition was 99.995%. More details about the sample preparation can be found elsewhere.^{23,24} To prevent the degradation of the EuO_{1-x} films when exposed to air, some films were protected by a Pt capping layer deposited in situ. The magnetic properties of both oxygen-deficient and stoichiometric EuO were examined using a physical properties measurement system (PPMS) from Quantum Design. X-ray diffraction (XRD) and scanning electron microscopy with energy dispersive x-ray spectroscopy (SEM-EDX) were used to investigate the films and verify they are of single phase fcc rock salt crystal structure.

III. RESULTS AND DISCUSSION

We have successfully developed a method to prepare EuO films based on pulsed laser deposition as referenced in [23,24]. XRD patterns show the stacking planes of the films are mostly aligned with the (200) lattice planes, same as reported from prior works.^{18,26} For oxygen-deficient EuO films, the normalized magnetization M as a function of temperature T (Fig. 1) shows that the Curie temperature is much enhanced beyond the intrinsic T_c of stoichiometric EuO of 69 K. Although M is relatively small above 69 K and the so called double-dome feature is not as pronounced as those reported elsewhere,^{15,16, 23-25} one still sees clearly the onset of the magnetic ordering near $T = 140$ K (see Fig. 1, inset (a)). To reveal more details of the temperature dependence of the magnetization, we also plot the magnetization in the logarithmic scale as a function of temperature in Fig. 1, inset (b). The double-dome feature is apparent. We will discuss the reason later in the paper why we focus on this sample, not the samples showing double-domes in the linear M - T plot studied in our previous investigations.²⁴

Figure 2(a) shows the magnetization as a function of applied magnetic field H (M - H) at different temperatures ($T = 5 - 120$ K). The M - H curves characteristic of a ferromagnet are seen over the entire temperature range shown. Although the saturation magnetization is significantly reduced near and above the intrinsic Curie temperature of the stoichiometric EuO $T_c = 69$ K, open hysteresis loop with a coercivity of 10 Oe persists at a temperature of 120 K. This can also be seen from Fig. 2(b), in which the coercivity H_c obtained from Fig. 2(a) is plotted as a function of temperature. A very unique feature is seen in Fig. 2(b): the coercive force first decreases as the temperature increases when $T < 69$ K, reaches almost zero near 69 K, then increases to a maximum as T continues to increase, and finally decreases and becomes zero again as the sample becomes paramagnetic ($T > 140$ K, not shown). Figure 2(c) shows the details of the M - H curves in the low field region for 40 K $< T < 100$ K.

The mechanism for the magnetic ordering at temperatures higher than 69 K is a matter of debate. One explanation suggested by Mauger⁴ is that doped electrons can be excited into the conduction band, which will effectively enhance the magnetic coupling between Eu^{2+} 4f local moments via 5d conduction electrons due to the 4f-5d exchange interaction (RKKY). One expects similar values of the saturation magnetization both below and above 69 K based on this local moment model. Alternative models based on exchange splitting of the conduction electrons²⁹ or magnetic polarons,³¹ however, predicts a smaller magnetization above 69 K. It suggests a much reduced contribution from the Eu^{2+} moments until the temperature is lowered below 69 K.^{15,16,23-25} As shown in Fig. 2(a), there is a big difference in the saturation magnetization for temperatures below and above 69 K. The magnetization is attributed to two different sources below and above 69 K. Below 69 K, the indirect exchange interaction between localized Eu^{2+} 4f spins is strong, which aligns their moments. The alignment of these local moments gets weaker as the temperature approaches 69 K. Above 69 K, we believe the doped electrons in their defect states form magnetic polarons with the nearby local Eu spins, as will be discussed later. The field dependence of M shown in Fig. 2(c) and the unique Hc-T curve shown in Fig. 2(b) suggest that the coupling between the local Eu moments of the Heisenberg ferromagnetic below 69 K and the moments of magnetic polaron is antiferromagnetic. The magnetic polaron state exists even below 69 K (over a certain temperature range), and their moments are coupled antiferromagnetically with the much larger local moments of the Eu, which dominates the magnetization at low temperature. The coercivity Hc initially decreases with increasing temperature due to reduced magnetic anisotropy that holds the Eu moments in the direction of magnetization, at the same time, M also decreases with the temperature. Close to 70 K, the Eu moments decrease to the level that is nearly canceled by the moments of the magnetic polarons. The M-H curve runs through the origin and Hc drops to zero. As the temperature increases further ($T > 70$ K) the magnetic polaron state dominates the magnetization, and the coercivity is finite again before it decreases to zero as the

magnetic order vanishes near 140 K.

To verify our postulate, we have examined in detail the hysteresis loops over the temperature range of interest, as shown in Figs. 3 and 4. At 60 K, shown in the inset (a) of Fig. 3, the hysteresis loop is that of a normal ferromagnet, although sign of narrowing in small fields is already seen. The local moments from Eu^{2+} 4f spins are much larger than the antiferromagnetically coupled moments of the magnetic polarons. When T is increased to 68 K, an inverted loop appears. The magnetization reverses its direction when the applied field is still positive as H is lowered from high positive field. Similar process occurs as H is swept from negative fields to positive fields. This inverted hysteresis loop strongly supports our interpretation that the local Eu moments are antiferromagnetically coupled to that of the magnetic polarons, which switches the former without applying a negative field. Being close to the ordering temperature of the local Eu moments, the magnetic anisotropy for Eu is small (H_c is close to zero) and the antiferromagnetic coupling is relatively weak. A large field aligns both subsets of the moments in the same direction. When the field decreases to a critical value, the local Eu moments reverse their direction due to the influence of the magnetic polarons. The latter do not reverse their direction and are quite stable because it is far below their ordering temperature of 140 K. Similar situation occurs when temperature goes up to 71 K. As shown in the inset (b) of Fig. 3, a smaller inverted loop appears compared to that at 68 K because of the much smaller Eu local moments' contribution to the measured magnetization. The vertical arrows in the plot indicate the orientation of the magnetic moments of each subset as the hysteresis curve crosses each other at various points of the loop. The inverted hysteresis loop disappears, and the M-H curve runs through the origin when temperature increases to 72 K, as shown in Fig. 4(a). This corresponds to the situation when the Eu local moments have decreased to a value that is canceled by the moments of the magnetic polarons near zero field. The antiferromagnetic coupling is weak at this temperature. The trend of the weakening of the coupling strength as T increases from 68 to 72 K can be seen in Figs 3, 3(b) and 4(a). They show progressively decreasing fields

where the coupling-induced switching of the Eu local moments occurs. The weakening of the coupling strength is consistent with the diminishing spontaneous magnetization as the system approaches the ordering temperature of the local Eu moments. Above 72 K the contribution from the Eu local moments is very small, and the magnetization from the magnetic polarons is now larger. The hysteresis loop becomes normal again (Fig. 4(b)).

Back to the question we mentioned in the first part of this section, the reason we can clearly see the inverted hysteresis loops from this sample is its relatively small magnetization above 69 K from the magnetic polarons. For the heavily oxygen-deficient EuO samples, M of the magnetic polarons is large and overwhelms the local Eu moments near the ordering temperature of the Eu. To go down to the temperature where the local moment is larger than the magnetic polarons, the magnetic anisotropy holding the Eu moments is larger than that of the magnetic polarons. Instead of being switched by the coupling to the magnetic polarons, the moments of the magnetic polarons themselves are switched. In both of these cases normal hysteresis loops are observed. Figure 5 shows the H_c - T curve for a heavily oxygen deficient sample. It does not exhibit near zero coercivity in the vicinity of 70 K. The interplay between the anisotropies of the two magnetic subsets as well as the coupling between the two may be complex and is an interest subject for future investigation. Determining the exact amount of oxygen vacancies in the films is difficult. However, the lattice constants ($a = 0.5131$ nm, 0.5116 nm and 0.5108 nm for the stoichiometric, lightly and heavily oxygen deficient films, respectively) are consistent with the expected degree of reduction.

The unique features in the magnetization, hysteresis and H_c - T curves provide strong evidence that the two subsets of magnetic moments, one dominant below and the other above 69 K, are antiferromagnetically coupled. The most plausible mechanism for the magnetic order above 69 K is magnetic polarons. Magnetic polaron model has been proposed for EuO early on and recently.^{31,32,37,38}

Experimental evidence for the presence of magnetic polarons has been shown in Raman scattering,³⁹ muon spin relaxation,⁴⁰ optical absorption,⁴¹ and NMR⁴² studies. Magnetic polaron was interpreted as a possible origin of the spatial inhomogeneity of the electronic structure in electron-doped EuO films observed in infrared magneto-optical imaging.⁴³ The electric, magnetic, and electron paramagnetic resonance data were also analyzed in a bound magnetic polaron model.⁴⁴ In our samples, the doped electrons are trapped in the defect levels associated with the oxygen vacancies and form bound magnetic polarons with the nearby Eu 4f spins. These magnetic polarons have fairly large diameters due to the high dielectric constant of EuO and overlap to a certain degree to form a ferromagnetically ordered state below 140 K; on the other hand, the mobility of the charge carriers remains low. This is consistent with the high resistivity of the samples. Recent results of angular-resolved photoemission spectroscopy on Gd and Ce doped EuO show filling of electron pockets in an otherwise empty conduction band, which is not observed in undoped EuO_{1-x} presented here.^{24,45} This further suggests bound magnetic polaron is a more appropriate model than models based on exchange-split conduction bands or RKKY interaction to describe the magnetic ordering of EuO_{1-x} above 69 K, although it is not to say magnetic polarons do not exist in Gd and Ce doped EuO. Since the Eu local spins are fully aligned only at the very low temperature, the magnetic polaron state can be stable below 69 K extending over quite a large temperature range. When the magnetic polarons finally collapse, the antiferromagnetic arrangement of the two subsets of the magnetization vanishes. One should see an increase in the M (T) at the lowest temperatures. Indeed, as shown in Fig. 1, a sudden increase in M is apparent as the temperature is lowered to about 20 K. The magnetization below 20 K is the sum of the Eu local moments and the doped electrons located in the majority conduction band that are no longer bound to the nearby Eu²⁺. The sudden increase in M is also seen in the heavily oxygen deficient sample shown in Fig. 5(a), but absent in stoichiometric EuO (Fig. 5(b)), which strongly supports the presence of magnetic polaron state in EuO_{1-x} that is coupled antiferromagnetically to the local Eu 4f moments ordered in the Heisenberg

ferromagnet. Interestingly, recent NMR investigation reveals that the magnetic inhomogeneity increases rapidly above 30 K in Gd doped EuO, which may signal the onset of the magnetic polaron state.⁴² In addition, infrared magneto-optical imaging shows spatial inhomogeneity due to phase separation at temperatures much below T_c .⁴³

In order to understand why the two subsets of the magnetization are aligned antiparallel to each other, we consider the following. Since the 4f orbital of Eu^{2+} is half-filled, a doped electron bound to the defect level will align the spins of the neighboring Eu^{2+} ions antiparallel to its own spin to form a magnetic polaron.⁴⁶ The conduction band is exchange split and the majority states are lowered although they have not crossed the defect level, at least for temperatures not too far below 69 K. Hybridization between the defect states and the conduction band favors that the doped electrons align their spins in the same direction as the majority states,³⁵ that is, in the same direction as those Eu local spins ordered in the Heisenberg ferromagnet. This argument assumes that the defect levels are not exchange split as suggested by Sinjukow and Nolting.³⁵ The net result is the antiferromagnetic coupling between the magnetic polarons (mostly from Eu) and the Eu local moments ordered in the Heisenberg ferromagnet. As the temperature is lowered, the Eu local moments are strongly aligned and the magnetic polaron state becomes energetically unfavorable. At the same time, the majority states of the conduction band cross the defect level and the doped electrons are in the conduction band. Figure 6 shows the schematics of the relationship between the ordered bound magnetic polaron state stable between 20 - 140 K and the Heisenberg ferromagnet dominant below 69 K.

It should be mentioned that the magnetic interaction that forms magnetic polarons has the tendency to localize the electrons around the oxygen vacancies³⁸ and delays the metal-insulator transition. Also to be noted is that the antiferromagnetic coupling discussed in this paper provides a satisfactory explanation for the apparent contradiction that electron doping increases T_c and, at the same time, reduces the red shift in the optical absorption, which implies a decrease in the ferromagnetic

coupling.^{47,48} We have focused on magnetic polarons here. Models based on exchange splitting of the conduction electrons have difficulty in producing the antiferromagnetic coupling and may require rare earth doping to achieve $T_c > 69$ K.^{29,49} The magnetic polaron model can also explain why most oxygen deficient samples show onset of the ferromagnetic ordering more or less near 140-150 K regardless the concentration of the oxygen vacancies. The Curie temperature is primarily determined by the coupling strength within an individual magnetic polaron. The concentration affects when the percolation of the magnetic polarons leads to a ferromagnetically ordered state and the total magnetization.

IV. CONCLUSIONS

In summary, we have observed antiferromagnetic coupling between the Eu 4f local moments ordered below $T_c = 69$ K and the magnetic polarons that is responsible for the ordering above 69 K in oxygen-deficient EuO_{1-x} thin films. Unique temperature dependent hysteresis, coercivity and magnetization support the conclusion. The magnetic polaron state is stable below 69 K and may persist down to 20 - 30 K. We suggest a model for the relative spin orientations of the doped electrons and Eu moments in the magnetic polarons and in the Heisenberg ferromagnet that explains the observed antiferromagnetic coupling. There are other implications of our finding as discussed.

ACKNOWLEDGEMENTS

This work was supported by the National Science Foundation (DMR-0852862 and CBET-0754821).

REFERENCES

- ¹B. T. Matthisa, R. M. Bozorth, and J. H. Van Vleck, Phys. Rev. Lett. **7**, 160 (1961).
- ²W. Heisenberg, Z. Phys. **49**, 619 (1928).
- ³J. H. van Vleck, J. Chem. Phys. **6**, 105 (1938).
- ⁴A. Mauger and C. Godart, Phys. Rep. **141** 51(1986).
- ⁵N. Tsuda, K. Nasu, A. Fujimori, and K. Siratori, Electronic Conduction in Oxides, Springer Series in Solid-State Sciences (Springer, New York, 2000).
- ⁶F. Lévy, Physik Kondens. Materie **10**, 71 (1969).
- ⁷M. R. Oliver, J. O. Dimmock, A. L. McWhorter, and T. B. Reed, Phys. Rev. B **5** 1078 (1972).
- ⁸Y. Shapira, S. Foner, R. L. Aggarwal, and T. B. Teed. Phys. Rev. B **8** 2316 (1973).
- ⁹K. Y. Ahn and J. C. Suits, IEEE Trans. Magn. MAG-3, 453 (1967).
- ¹⁰P. G. Steeneken, L. H. Tjeng, I. Elfimov, G. A. Sawatzky, G. Ghiringhelli, N. B. Briikes, and D. J. Huang, Phys. Rev. Lett. **88** 047201 (2002).
- ¹¹D. Dimarzio, M. Croft, and N. Sakai, Phys. Rev. B **35**, 8891 (1987).
- ¹²V. G. Tissen and E. G. Ponyatovskii, JETP Lett. **46**, 361 (1988).
- ¹³W. Söllinger, W. Heiss, R. T. Lechner, K. Rumpf, P. Granitzer, H. Krenn, and G. Spingholz, Phys. Rev. B **81**, 155213 (2010).
- ¹⁴N. J. C. Ingle and I. S. Elfimov, Phys. Rev. B **77**, 121202 (R) (2008).
- ¹⁵A. S. Borukhovich, V. G. Bamburov, and A. A. Sidorov, J. Magn. Mater. **73** 1 (1988).
- ¹⁶T. Matsumoto, K. Yamaguchi, M. Yuri, K. Kawaguchi, N. Koshizaki, and K. Yamada. J. Phys. Condens. Matter **16** 6017 (2004).
- ¹⁷H. Ott, S. J. Heise, R. Sutarto, Z. Hu, C. F. Chang, H. H. Hsieh, H.-J. Lin, C. T. Chen, and L. H. Tjeng, Phys. Rev. B **73**, 094407 (2006).
- ¹⁸A. Schmehl, V. Vaithyanathan, A. Herrnberger, S. Thiel, C. Richter, M. Liberati, T. Heeg, M. Röckerath, L. F. Kourkoutis, S. Mühlbauer, P. Böni, D. A. Müller, Y. Barash, J. Schubert, Y. Idzerda, J. Mannhart, and D. G. Schlom, Nature Mater. **6** 882 (2007).
- ¹⁹R. Sutarto, S. G. Altendorf, B. Coloru, M. Moretti Sala, T. Hauptrecht, C. F. Chang, Z. Hu, C. Schüßler-Langeheine, N. Hollmann, H. Kierspel, J. A. Mydosh, H. H. Hsieh, H.-J. Lin, C. T. Chen, and L. H. Tjeng, Phys. Rev. B **80**, 085308 (2009).
- ²⁰H. Miyazaki, H. J. Im, K. Terashima, S. Yagi, M. Kato, K. Soda, T. Ito, and S. Kimmura, Appl.

- Phys. Lett. **96** 232503 (2010).
- ²¹T. Mairoser, A. Schmehl, A. Melville, T. Heeg, L. Canella, P. Böni, W. Zander, J. Schubert, D. E. Shai, E. J. Monkman, K. M. Shen, D. G. Schlom, and J. Mannhart, Phys. Rev. Lett. **105**, 257206 (2010).
- ²²T. Mairoser, A. Schmehl, A. Melville, T. Heeg, W. Zander, J. Schubert, D. E. Shai, E. J. Monkman, K. M. Shen, T. Z. Regier, D. G. Schlom, and J. Mannhart, Appl. Phys. Lett. **98**, 102110 (2011).
- ²³X. Wang, P. Liu, K. A. Fox, J. Tang, J. Colón Santana, K. Belashchenko, P. Dowben, and Y. Sui, IEEE Tran. On Mag. **46** 6 (2010).
- ²⁴P. Liu, J. Tang, J. Colón Santana, K. D. Belashchenko, and P. Dowben, J. Appl. Phys. **109**, 07C311 (2011).
- ²⁵M. Barbagallo, N. D. M. Hine, J. F. K. Cooper, N.-J. Steinke, C. H. W. Barnes, C. J. Kinane, R. M. Dalgliesh, T. R. Charlton, and S. Langridge, Phys. Rev. B **81**, 235216 (2010).
- ²⁶J. Lettieri, V. Vaithyanathan, S.K. Eah, J. Stephens, V. Sih, D.D. Awschalom, J. Levy, and D.G. Schlom, Appl. Phys. Lett., **83** 975 (2003).
- ²⁷R. P. Panguluri, T. S. Santos, E. Negusse, J. Dvorak, Y. Idzerda, J. S. Moodera, and B. Nadgorny, Phys. Rev. B **78**, 125307 (2008).
- ²⁸A. G. Swartz, J. Ciraldo, J. J. I. Wong, Y. Li, W. Han, T. Lin, S. Mack, J. Shi, D. D. Awschalom, and R. K. Kawakami, Appl. Phys. Lett. **97**, 112509 (2010).
- ²⁹M. Arnold and J. Kroha, Phys. Rev. Lett. **100**, 046404 (2008).
- ³⁰A. Mauger, Phys. Status Solidi B. **84**, 761 (1977).
- ³¹J. B. Torrance, M. W. Shafer, and T. R. McGuire, Phys. Rev. Lett. **29**, 1168 (1972).
- ³²W. Nolting, S. Mathi Jaya, and S. Rex, Phys. Rev. B **54**, 14455 (1996).
- ³³A. C. Durst, R. N. Bhatt, and P. A. Wolff, Phys. Rev. B **65**, 235205 (2002).
- ³⁴U. Yu and B. I. Min, Phys. Rev. Lett., **94**, 117202 (2005).
- ³⁵P. Sinjukow and W. Nolting, Phys. Rev. B **68**, 125107 (2003).
- ³⁶S. G. Altendorf, A. Efimenko, V. Oliana, H. Kierspel, A. D. Rata, and L. H. Tjeng, Phys. Rev. B **84**, 155442 (2011).
- ³⁷J. Kübler and D. T. Vigen, Phys. Rev. B **11**, 4440 (1975).
- ³⁸A. Mauger, Phys. Rev. B **27**, 2308 (1983).

- ³⁹H. Rho, C. S. Snow, S. L. Cooper, Z. Fisk, A. Comment, and J-Ph Ansermet, Phys. Rev. Lett. **88**, 127401 (2002).
- ⁴⁰V. G. Storchak, D. G. Eshchenko, E. Morenzoni, N. Ingle, W. Heiss, T. Schwarzl, G. Springholz, R. L. Kallaher, and S. von Molnár, Phys. Rev. B **81**, 153201 (2010).
- ⁴¹J. P. Lascaray, J. P. Desfours, and M. Averous, Solid State Commun. **19**, 677 (1976).
- ⁴²A. Comment, J. Ansermet, C. P. Slichter, H. Rho, C. S. Snow, and S. L. Cooper, Phys. Rev. B **72**, 014428 (2005).
- ⁴³S. Kimura, T. Ito, H. Miyazaki, T. Mizuno, T. Iizuka, and T. Takahashi, Phys. Rev. B **78**, 052409 (2008).
- ⁴⁴O. Massenet, Y. Capiomont, and N. V. Dang, J. Appl. Phys. **45**, 3593 (1974).
- ⁴⁵J. A. Colón Santana, J. M. An, N. Wu, K. D. Belashchenko, X. Wang, P. Liu, J. Tang, Y. Losovyj, I. N. Yakovkin, and P. A. Dowben, Phys. Rev. B **85**, 014406 (2012).
- ⁴⁶J. M. D. Coey, M. Venkatesan, and C. B. Fitzgerald, Nature Mater. **4** 173 (2005).
- ⁴⁷J. Schoenes and P. Wachter, Phys. Rev. B **9**, 3097 (1974).
- ⁴⁸W. Nolting and A. M. Oleś, Z. Phys. B – Condensed Matter **43**, 37 (1981).
- ⁴⁹P. Sinjukow and W. Nolting, Phys. Rev. B **69**, 214432 (2004).

Figure Captions

FIG.1. Temperature dependence of normalized magnetization (M-T) of EuO_{1-x} . The applied magnetic field is 200 Oe. Inset (a) Enlarged view of the M-T curve in the dashed rectangular frame. Inset (b) Logarithmic scale of normalized magnetization as a function of temperature.

FIG. 2. (a) Magnetization as a function of applied field over the temperatures range from 5 K to 120 K for EuO_{1-x} . (b) Coercivity obtained from (a) as a function of temperature. (c) Details of the M-H curves in the low field region for $40 \text{ K} < T < 100 \text{ K}$.

FIG. 3. Enlarged view of magnetization as a function of applied field at 68 K. Inset (a): Enlarged view of magnetization as a function of applied field at 60 K; Inset (b): Enlarged view of magnetization as a function of applied field at 71 K. The arrows superimposed on the curves show the directions of the field sweep. The vertical arrows indicate the direction of the magnetic moments at the corresponding regions of field: green for local Eu moments, and purple for magnetic polarons.

FIG. 4. (a) Enlarged view of magnetization as a function of applied field at 72 K; the inset shows a detailed view near zero field. (b) Enlarged view of magnetization as a function of applied field at 80 K. The arrows superimposed on the curves show the directions of the field sweep.

FIG. 5. Coercivity as a function of temperature for a heavily oxygen-deficient EuO sample. Inset (a): Magnetization as a function of temperature for the heavily oxygen-deficient EuO sample. Inset (b): Magnetization as a function of temperature for a stoichiometric EuO sample.

FIG. 6. Schematics of the relationship between the ordered magnetic polaron state stable between 20 K - 140 K and the Heisenberg ferromagnet dominant below 69 K.

FIG. 1.

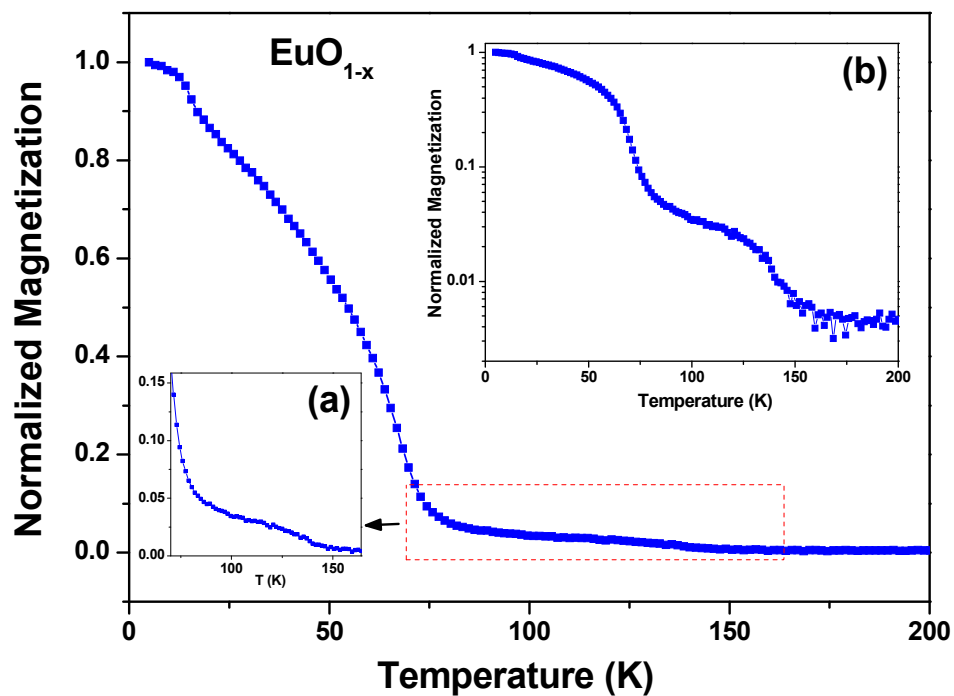


FIG. 2.

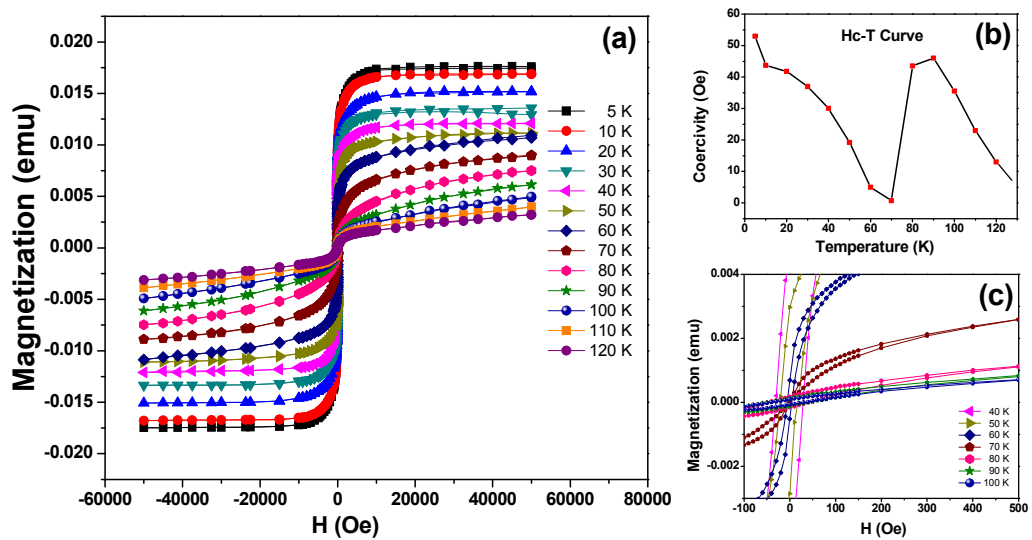


FIG. 3.

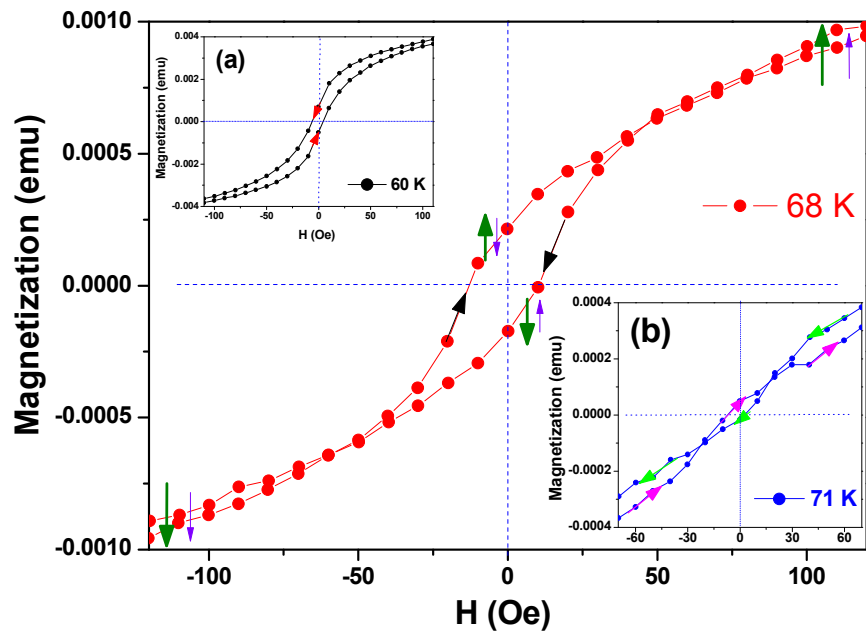


FIG. 4.

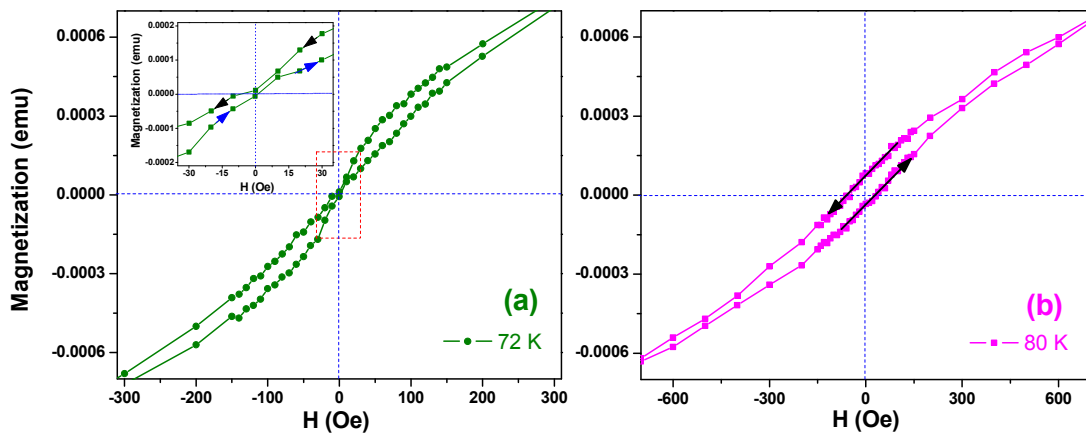


FIG. 5.

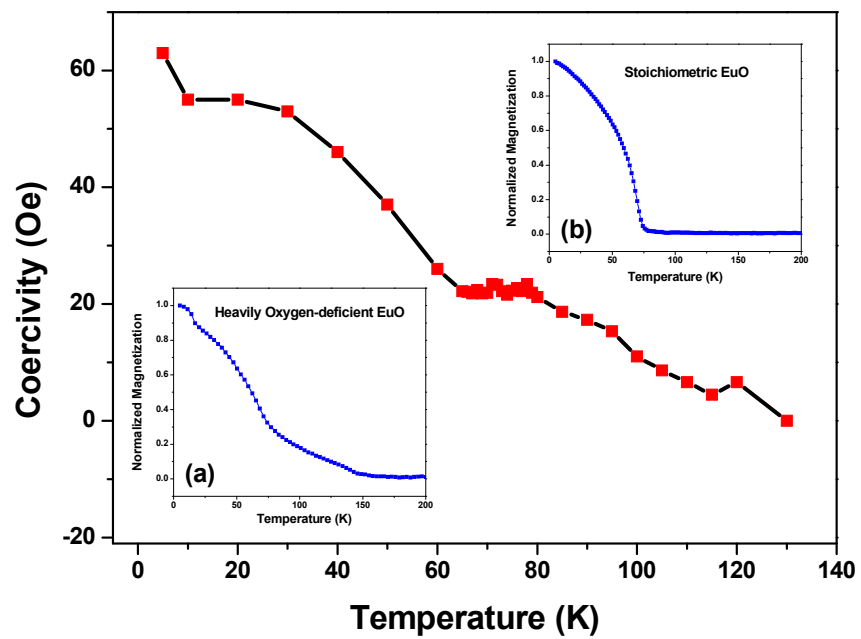


FIG. 6.

